A Simple Conducted Noise Modeling Method for DC-DC Converters with Accurate Noise Source Model

ZHANG, Baihua
Department of Electrical and Electronic Engineering, Graduate School of Information Science and Electrical Engineering, Kyushu University : Graduate Student

ZHANG, Shuaitao
Department of Electrical and Electronic Engineering, Graduate School of Information Science and Electrical Engineering, Kyushu University : Graduate Student

SHOYAMA, Masahito
Department of Electrical Engineering, Faculty of Information Science and Electrical Engineering, Kyushu University

TAKEGAMI, Eiji
TDK-Lambda Corporation

https://doi.org/10.15017/2195854

出版情報：九州大学大学院システム情報科学紀要. 24 (1), pp.9-15, 2019-01-25. Faculty of Information Science and Electrical Engineering, Kyushu University
バージョン：
権利関係：

九州大学大学院
システム情報科学紀要
第 24 巻　第 1 号　平成 31 年 1 月

Research Reports on Information Science and
Electrical Engineering of Kyushu University
Vol.24, No.1, January 2019

A Simple Conducted Noise Modeling Method for DC-DC Converters with Accurate Noise Source Model

Baihua ZHANG*, Shuaitao ZHANG*, Masahito SHOYAMA** and Eiji TAKEGAMI***

(Received November 21, 2018)

Abstract: In this study, a simple conducted noise modeling method based on classical frequency domain modeling concept is developed. Compared with conventional methods, the accuracy of noise source model in the proposed modeling method is improved by using S-shape waveform model with the consideration of high frequency ringing waveforms. The parameters of noise source model are extracted on the basis of experimental measured waveforms. Finally, the accuracy of the proposed conducted noise modeling method is validated on a DC-DC boost converter, the comparison between measured and calculated conducted noise spectra show that the low frequency (0.15 MHz-2 MHz) noise peaks as well as high frequency (10 MHz-30MHz) peak can be accurately predicted.

Keywords: EMI modeling, Conducted noise, Fourier transform, DC-DC converters

1. Introduction

Switching power converters tend to become more and more compact and lightweight with the increase of switching frequency, owing to the development of semiconductor devices and power electronics techniques. The conducted emission associated with fast switching actions also tends to increasingly introduce interferences to power conversion systems. Therefore, electromagnetic interference (EMI) modeling is a significant work that facilitates the possibility to efficiently solve EMI problem and design EMI filters[1].

The current EMI noise modeling methods can be divided into two groups including time domain and frequency domain modeling methods, they all have their own strengths and weakness comparing with each other. The time domain modeling method also called as lumped circuit model is an extremely nature method that based on the physics of the actual circuit. The lumped circuit model is implemented in software simulated in time domain and finally transformed to frequency domain by fast Fourier transform (FFT) analysis. In lumped circuit model, every detail should be taken into consideration including switching device models and passive components like resistances, inductances and capacitances. In addition, the parasitic components on imperfect devices, cables and printed circuit board (PCB) should also be included in the model. Therefore, with the increase of the number of the components and complexity of the circuit, the model becomes complex and it is hard for simulation to reach convergence state. Thus, the time domain modeling method is time-consuming and requires large computational resources. It is also difficult to create the accurate noise model without deep understanding of all the devices and components[2,3].

The frequency domain method is also called as behavior modeling method that based on noise source and noise propagation path concepts. The conventional frequency domain method is the simplest method that the characteristics of noise source and noise propagation path are presented in frequency domain and then the noise spectrum can be predicted in a simple and fast way[4)-6)]. However, the conventional frequency domain method suffers from the inaccuracy of high frequency range noise modeling. In recent years, a series of novel terminal modeling methods are proposed that treat converters as “black box”. On the basis of the observation of a set of port voltage and current, the conducted emission characterizations of the converter is modeled by a Thevenin or Norton equivalent circuit without considering the actual structure and components inside[4)-12)]. The terminal modeling methods are able to be applied for system level conducted noise modeling, and also show a perfect accuracy, which are helpful for the EMI filters designs. However, the “black box” used in terminal modeling method is unable to indicate the essential of the conducted emission problem. The understanding of the noise source and noise propagation path is so vogue that cannot be considered a useful modeling method to help with the solution to noise problem from where it is generated.

*　Department of Electrical and Electronic Engineering, Graduate Student
**　Department of Electrical Engineering
***　TDK-Lambda Corporation

In this study, on the basis of conventional frequency domain molding concepts, a simple frequency domain EMI noise modeling method is proposed. The accuracy of high frequency range noise modeling is improved by proposed accurate noise source model, which is the weakness of the classical frequency domain modeling method.

In this study, a DC-DC boost converter is taken as an example to illustrate the proposed conducted noise modeling method. At first, the common mode (CM) noise model and propagation path are analyzed, and then the simple conducted noise spectrum expression in frequency domain is presented. Then, the Fourier coefficients of the noise sources are modeled on basis of experimental measured waveforms, and also the accuracy is verified by inverse Fourier transform. Finally, the comparison of predicted and measured conducted noise spectra are given to validate the effectiveness of the proposed simple noise modeling method.

2. Noise Model of DC-DC Boost Converter

Figure 1 shows the schematic of a boost converter with line impedance stabilization network (LISN). Capacitor C_p is additional added to function as the typical parasitic capacitor between the drain of the MOSFET and frame ground in practical applications.

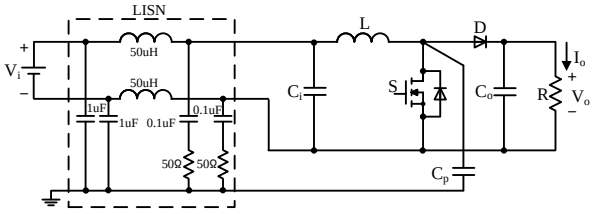

Fig. 1. Boost converter with LISN.

Figure 2(a) shows the common mode (CM) noise generation mechanism, the fast turn-on and turn-off operations of switch S cause the occurrence of the high frequency EMI noise. Then, as the noise propagation path shown in **Fig. 2(a)**, the noise current flows through parasitic capacitor C_p which provide a relevant low impedance propagation, and then flows into LISN and finally back to the switch. **Figure 2(b)** shows the equivalent circuit of CM noise model, the input capacitor C_i is regarded as short in high frequency range, and two paralleled 50 Ohm resistors in LISN is represented as a 25 Ohm resistor. The voltage V_{ds} that across the switch S is modeled as the noise source V_n in the equivalent circuit.

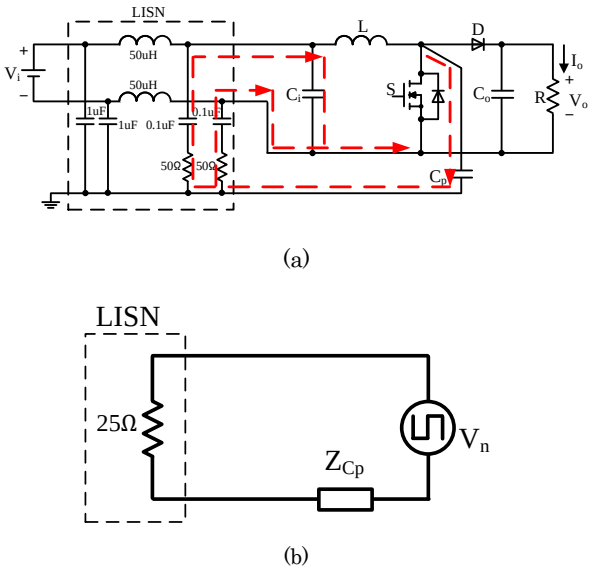

Fig. 2. CM noise in boost converter (a) noise propagation path, (b) equivalent circuit.

The CM noise current flows into frame ground via C_p and finally picked up by two paralleled 50 Ohm resistors in LISN as shown in **Fig. 2(a)**. Accordingly, the CM noise voltage measured by LISN can be calculated by equation (1), the Z_{Cp} is the impedance of capacitor C_p.

$$V_{cm}(f) = \frac{25}{25 + Z_{Cp}(f)} \cdot V_n(f) \quad (1)$$

The propagation path of differential mode (DM) is shown in **Fig. 3**, the noise current flows through inductor L and LISN and finally back to noise source. As the noise source is series with an inductor which has high impedance in the high frequency range, and parallel with input capacitor C_i which has a low impedance in high frequency range, the DM noise that picked up by LISN is regarded as relevant small comparing with the CM noise. Thus indicating that the CM noise is considered as dominant noise source, and results in the most contribution to the conducted noise spectrum of the boost converter. Therefore this research only focuses on the conducted CM noise modeling.

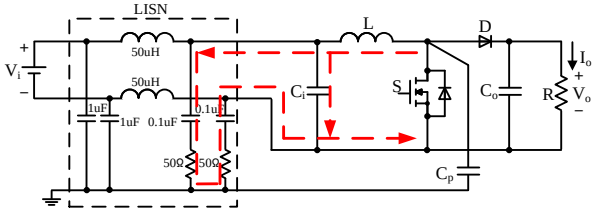

Fig. 3. DM noise propagation path in boost converter.

3. Accurate Noise Source Modeling

As previously mentioned, the voltage V_{ds} that across the switch is considered as CM noise source. Therefore, the noise source should be modelled on the basis of parameters of V_{ds} waveform, and then transformed from time domain to frequency domain by Fourier transform.

3.1. Square, Trapezoidal, and S-Shape Waveform Models

In conventional noise modeling methods, the noise voltage source is always modeled as a square waveform as shown in **Fig. 4(a)**. The square waveform model contains the information of amplitude A, period T_0 and duration τ. The trapezoidal waveform shown in **Fig. 4(b)** is also applied to model noise source, which contains more information of rise time τ_r and fall time τ_f than square waveform, and provides a more accurate model than square waveform model. However, compared with actual noise waveform, the trapezoidal waveform model still fails to include some important details.

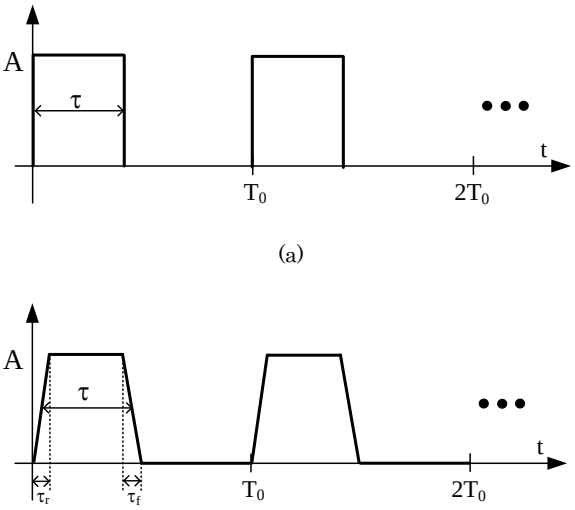

Fig. 4. Conventional noise source model (a) Square waveform; (b) Trapezoidal waveform.

In this study, an S-shape waveform model shown in **Fig. 5** is used for noise source modeling in order to include details as much as possible. The illustration of square, trapezoidal and S-shape waveforms is shown in **Fig. 6**[13], it is obvious that the S-shape waveforms include much more information than square and trapezoidal waveforms. Based on the illustration shown in **Fig. 6** and differentiation characteristics of Fourier coefficient expressed in equations (2) and (3). The Fourier coefficient of S-shape waveform is expressed in equation (4).

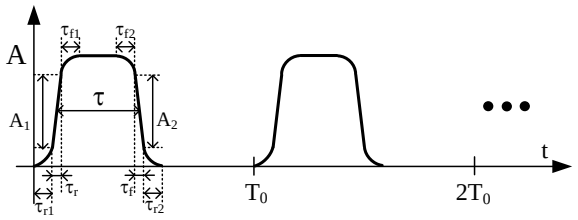

Fig. 5. S-shape waveform model.

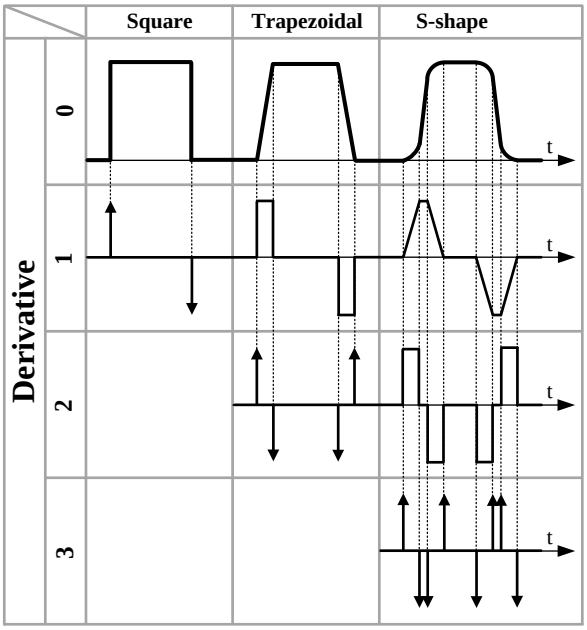

Fig. 6. Illustration of square, trapezoidal and S-shape waveforms[13].

$$\frac{d^k x(t)}{dt^k} = \sum_{n=-\infty}^{\infty} C_n \frac{d^k}{dt^k}\left(e^{jn\omega t}\right) = \sum_{n=-\infty}^{\infty} C_n (jn\omega)^k e^{jn\omega t} \quad (2)$$

$$C_n = \frac{C^{(k)}}{(jn\omega)^k} \quad (3)$$

$$C_{n\_S} = \frac{1}{(jn\omega_0)^3}\frac{1}{T_0}\left\{\frac{A_1}{\tau_r\tau_{r1}} - \frac{A_1}{\tau_r\tau_{r1}}e^{jn\omega_0\tau_{r1}} - \frac{A_1}{\tau_r\tau_{f1}}e^{jn\omega_0(\tau_{r1}+\tau_r)} + \frac{A_1}{\tau_r\tau_{r1}}e^{jn\omega_0(\tau_{r1}+\tau_r+\tau_{f1})}\right.$$
$$\left. - \frac{A_2}{\tau_f\tau_{f2}}e^{jn\omega_0\left(\tau_{r1}+\frac{1}{2}\tau_r+\tau-\frac{1}{2}\tau_f-\tau_{f2}\right)} + \frac{A_2}{\tau_f\tau_{f2}}e^{jn\omega_0\left(\tau_{r1}+\frac{1}{2}\tau_r+\tau-\frac{1}{2}\tau_f\right)} + \frac{A_2}{\tau_f\tau_{r2}}e^{jn\omega_0\left(\tau_{r1}+\frac{1}{2}\tau_r+\tau+\frac{1}{2}\tau_f\right)} - \frac{A_2}{\tau_f\tau_{r2}}e^{jn\omega_0\left(\tau_{r1}+\frac{1}{2}\tau_{r1}+\tau+\frac{1}{2}\tau_f+\tau_{r2}\right)}\right\} \quad (4)$$

$$C_{n\_reso} = \frac{A_{reso}}{j2T_0}\cdot e^{-jn\omega_0 t_{reso}}\left\{\frac{e^{(-jn\omega_0+j\omega_{reso}-k_{reso})\tau}-1}{-jn\omega_0+j\omega_{reso}-k_{reso}} - \frac{e^{(-jn\omega_0-j\omega_{reso}-k_{reso})\tau}-1}{-jn\omega_0-j\omega_{reso}-k_{reso}}\right\} \quad (5)$$

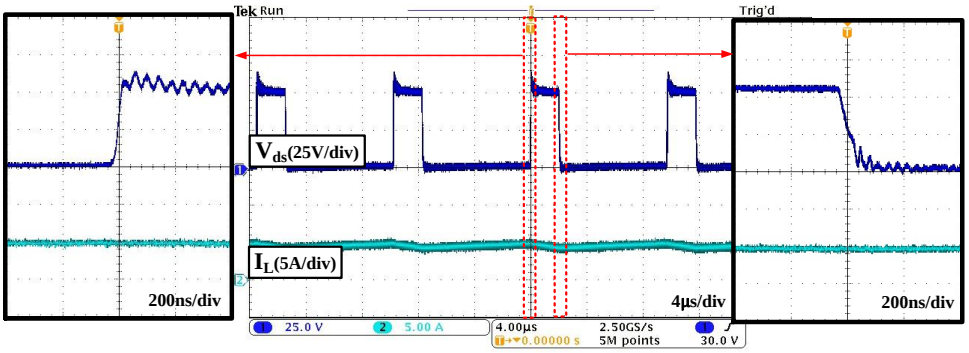

Fig. 8. Experimental waveforms.

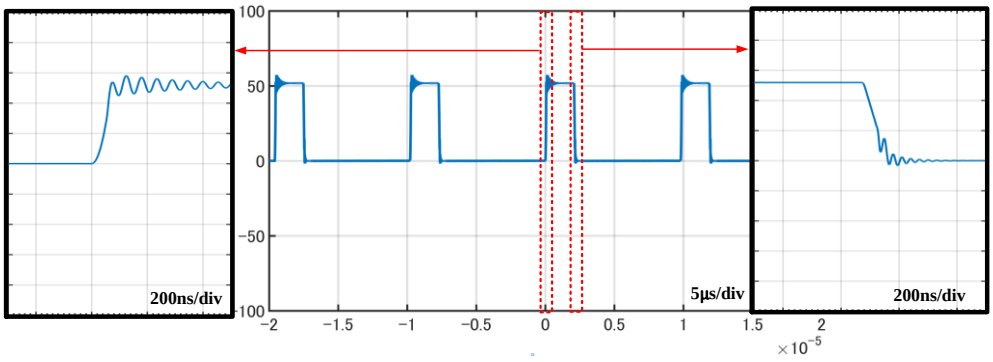

Fig. 9. Calculated waveforms.

3.2. Ringing Waveforms

Many parasitic components exist in the practical circuit including inductances, capacitances and resistances. Along with the fast switching actions of the switch, resonances occur owing to the existence of the parasitic components. The resonance waveform is also a part of noise source waveform with high frequency as shown in **Fig. 7**. The resonance waveforms are considered as noise sources that result in remarkable contribution to high frequency range noise on the conducted noise spectrum, therefore cannot be neglected.

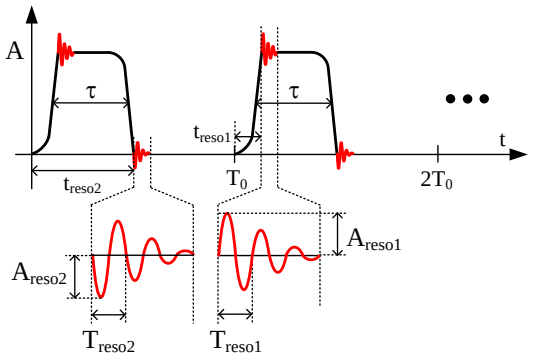

Fig. 7. S-shape waveform with ringing waveform.

The resonance waveforms are also taken into consideration in the proposed noise source model as shown in **Fig. 7**, and the Fourier coefficients of resonance waveforms are also derived on the basis of the parameters of waveforms to transform the expression from time domain to frequency domain. The final calculated Fourier coefficient of resonance waveforms is expressed in equation (5).

The sum of the Fourier coefficients of S-shape waveform and ringing waveforms is modeled as the expression of the noise source model in frequency domain, which contains information including amplitude, duration time, rise/fall time, and ringing waveforms, and is considered as an accurate noise source model. The experimental measurements are conducted on a boost converter implemented with the parameters listed in **Table 1**. The noise source model is created on the basis of the experimental measured V_{ds} waveform shown in **Fig. 8**. As even a small error may result in significant discrepancy of the calculated noise spectrum, the calculated Fourier coefficients are verified by inverse Fourier transform based on equation (6) to transform the noise source model from frequency domain to time domain, and then the waveforms in time domain can be

drawn. According to the comparison between the calculated waveform shown in **Fig. 9** and experimental measured waveform shown in **Fig. 8**, it comes to a conclusion that the accuracy of calculated Fourier coefficients of noise source model is verified.

$$V_{ds}(t) = \sum_{n=-\infty}^{\infty} C_n \cdot e^{jn\omega_0 t} \qquad (6)$$

Table 1 Circuit Parameters

Parameter	Symbol	Value
Input voltage	V_i	12 V
Output voltage	V_o	48 V
Switching frequency	f_s	103 kHz
Parasitic capacitor	C_p	1 nF

4. Experimental Verification

In the practical circuit, the parasitic components exist everywhere, including but not limited to the impedance of cable between the terminals of LISN and equipment under test (EUT), and parasitic impedance of the printed circuit board (PCB). Therefore the impedance of aforementioned parts are also taken into consideration and calculated as a part of the noise propagation path. The impedance components mentioned above are measured and added in the noise propagation path. The final CM noise model of boost converter is shown in **Fig. 10** with the noise source model and propagation path model, and the calculation expression is expressed in equation (7) accordingly, where the Z_{Cp} is the impedance of capacitor Cp, the Z_{Cable} is the sum of the impedance of the cable of LISN and input side cable of the converter; the Z_{PCB} is the impedance of the PCB.

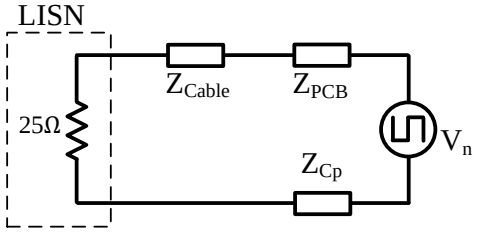

Fig. 10. Equivalent circuit of CM noise with parasitic components.

$$V_{cm}(f) = \frac{25}{25 + Z_{Cp}(f) + Z_{Cable}(f) + Z_{PCB}(f)} \cdot V_n(f) \qquad (7)$$

The proposed conducted noise modeling method is verified on a DC-DC boost converter with the circuit parameters listed in **Table 1**. Also the conducted noise spectrum is calculated based on the noise source and noise propagation path model expressed by equation (7). **Figure 11** shows the comparison between the experimental measured spectrum and predicted conducted noise spectrum envelope with conventional square waveform, trapezoidal waveform and proposed noise source models that shown in **Fig. 4 (a)**, **Fig. 4 (b)** and **Fig. 7** respectively. The red line and blue line are the calculated and experimental measured noise spectra. According to **Fig. 11 (a)** and **Fig. 11 (b)**, it can be found that the peaks in low frequency range (0.15 MHz-2 MHz) can be covered perfectly by calculated noise spectrum envelope which using conventional square waveform and trapezoidal waveform models, however these models are fail to match peak in the high frequency range (10 MHz-30 MHz) of the noise spectra. In **Fig. 11 (c)**, by applying the proposed noise source model, the peaks in the low frequency range (0.15 MHz-2 MHz) as well as the peak in high frequency range (10 MHz-30 MHz) can be covered perfectly by calculated noise spectrum envelope. Therefore, the calculated noise spectrum is in accordance with the measured spectrum, and the drawback of conventional frequency domain EMI modeling methods is improved by the noise source model proposed in this research.

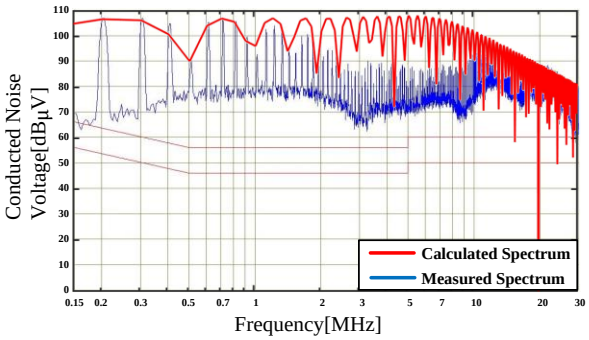

(a)

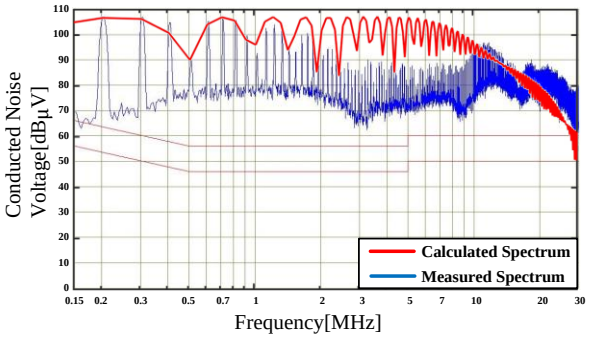

(b)

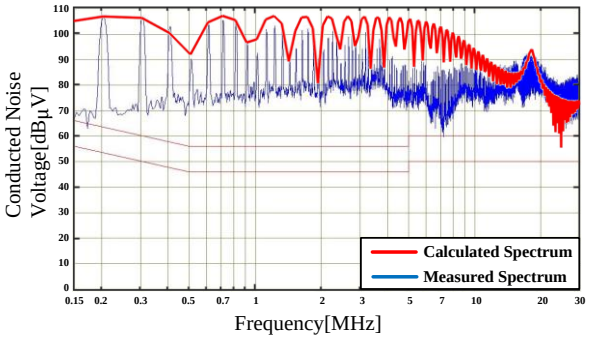

(c)

Fig. 11. Conducted noise spectrum with different noise source models (a) square waveform noise source model; (b) trapezoidal waveform noise source model; (c) proposed noise source model.

The generality of the proposed conducted noise modeling method is discussed by adding Y capacitors in the circuit as an EMI filter to change noise propagation path as the schematic and equivalent circuit shown in **Fig. 12(a)** and **(b),** where the Z_{Cable1} and the Z_{Cable2} are the impedance of the LISN and input cable of the converter. **Figure 13** shows the comparison of the calculated and measured conducted noise spectra with the conventional and proposed noise source models. The second peak in the high frequency range (10 MHz-30 MHz) of the noise spectra cannot be predicted by using conventional noise source models as shown in **Fig. 13 (a)** and **Fig. 13 (b)**. However, as shown in **Fig. 13 (c)**, by applying the proposed noise source model, the noise peaks in low frequency range (0.15 MHz-2 MHz) and high frequency range (10 MHz-30 MHz) in the experimental measured and calculated spectra match very well, the effectiveness of the proposed method is validated. Therefore the proposed conducted noise modeling method can be applied in different applications and topologies.

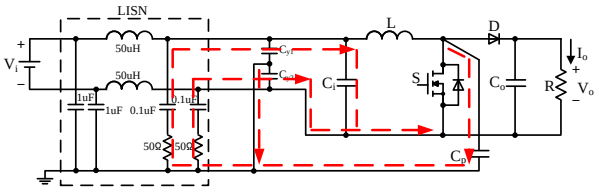

(a)

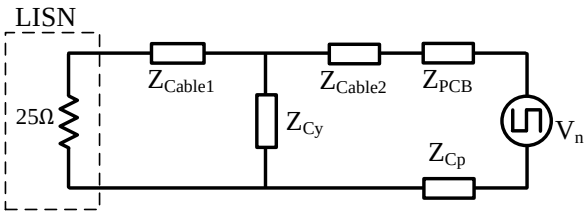

(b)

Fig. 12. CM noise in boost converter with Y capacitors, (a) noise propagation path; (b) equivalent circuit.

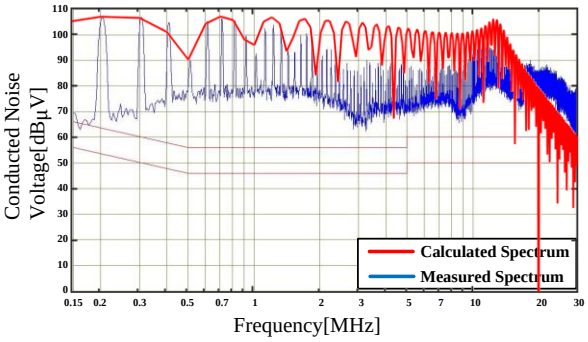

(a)

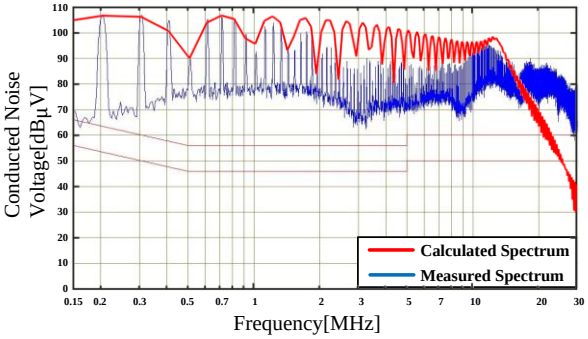

(b)

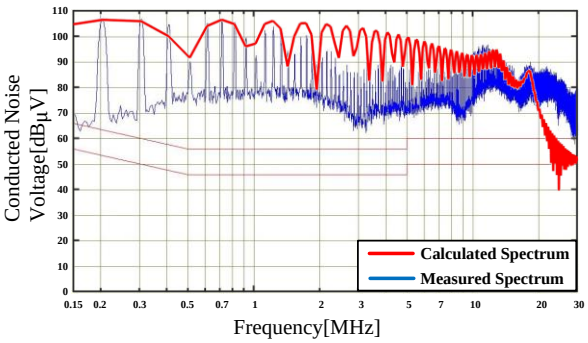

(c)

Fig. 13. Conducted noise spectrum after adding Y capacitors with different noise source models (a) square waveform noise source model; (b) trapezoidal waveform noise source model; (c) proposed noise source model.

5. Conclusion

A simple frequency domain conducted noise modeling method with an accurate noise source model is proposed in this study. The Fourier coefficients of the practical experimental measured noise source waveforms are calculated to transform the expression from time domain to frequency domain, which is an accurate noise source model with enough information. The accuracy of the noise source model is also verified by comparing the waveform of calculated noise source model with the original noise source waveform in time domain. Finally, the effectiveness of the proposed conducted noise modeling method is validated on a boost converter without and with an EMI filter added. The low frequency (0.15 MHz-2 MHz) and high frequency (10 MHz-30 MHz) conducted noise can be calculated perfectly by proposed noise modeling method.

References

1) Henry W. Ott, Electromagnetic Compatibility Engineering, Wiley, Chap. 1, 2009.
2) L. Yang, B. Lu, W. Dong, Zhiguo Lu, M. Xu, F. C. Lee and W. G. O. Odendaal, "Modeling and Characterization of a 1KW CCM PFC Converter for Conducted EMI Prediction," in *Proc. IEEE APEC'04*, pp. 1–7, 2004.
3) A. C. Baisden, D. Boroyevich and J. D. V. Wyk, "High Frequency Modeling of a Converter with an RF-EMI Filter," in *Proc. IEEE IAS'06*, pp. 2290–2295, 2006.
4) S. Wang, F. C. Lee and W. G. Odendaal, "Improving the Performance of Boost PFC EMI Filters," in *Proc. IEEE APEC'03*, pp. 368–374, 2003.
5) E. Gubia, P. Sanchis, A. Ursua, J. Lopez and L. Marroyo, "Frequency Domain Model of Conducted EMI in Electrical Drives," *IEEE trans. Power Electron.*, Vol. 3, No. 2, pp. 45–49, June 2005.
6) K. Maimali and R. Oruganti, "Simple Analytical Models to Predict Conducted EMI Noise in a Power Electronic Converter," in *Proc. IEEE IECON'07*, pp. 1930–1936, 2007.
7) Q. Liu, F. Wang and D. Boroyevich, "Modular-Terminal-Behavioral (MTB) Model for Characterizing Switching Module Conducted EMI Generation in Converter Systems," *IEEE trans. Power Electron.*, Vol. 21, No. 6, pp. 1804–1814, Nov. 2006.
8) Q. Liu, F. Wang and D. Boroyevich, "Conducted-EMI Prediction for AC Converter Systems Using an Equivalent Modular-Terminal-Behavioral (MTB) Source Model," *IEEE trans. Ind. Electron.*, Vol. 43, No. 5, pp. 1360–1370, Sep. 2007.
9) A. C. Baisden, D. Boroyevich and F. Wang, "Generalized Terminal Modeling of Electromagnetic Interference," *IEEE trans. Ind. Electron.*, Vol. 43, No. 5, pp. 2068–2079, Sep. 2010.
10) H. Bishnoi, P. Mattavelli, R. Burgos and D. Boroyevich, "EMI Terminal Modeling of DC-Fed Motor Drives," in *Proc. EPE'07 ECCE Europe*, pp. 1–10, 2013.
11) B. Sun and R. Burgos, "Assessment of Switching Frequency Impact on the Prediction Capability of Common-Mode EMI Emissions of SiC Power Converters Using Unterminated Behavioral Models," in *Proc. IEEE APEC'15*, pp. 1153-1160, 2015.
12) M. Prajapati and K. Y. See, "Extraction of Equivalent Noise Model From Photovoltaic Systems," *IEEE trans. Electromagn. Compat.*, early accept, 2018.
13) S. Walder, X. Yuan, I. Laird and J. J. O. Dalton, "Identification of the Temporal Source of Frequency Domain Characteristics of SiC MOSFET Based Power Converter Waveforms," in *Proc. IEEE ECCE'16*, pp. 1–8, 2016.